NASA Contractor Report 165325

THE IMPACT RESISTANCE OF SiC AND OTHER MECHANICAL PROPERTIES OF SiC AND Si_3N_4

Richard C. Bradt

The Pennsylvania State University

University Park, Pennsylvania 16802

April 1984

Prepared for

NATIONAL AERONAUTICS AND SPACE ADMINISTRATION
Lewis Research Center
Under Grant NSG-3016

TABLE OF CONTENTS

SUMMARY

This report summarizes the most important results of an extended study of the impact and other mechanical properties of commercial SiC materials. The mechanical properties of two Si_3N_4 materials were investigated as well. The first two portions of this study were focused on the impact resistance of a number of silicon carbides as tested in an instrumented Charpy system, initially at room temperature, then extended to elevated temperatures of 1500°C and above. Creep studies of several of these silicon carbides were also completed. Other studies involved the dynamic fatigue and slow crack growth from 1000°C to 1400°C and also a study of the fracture statistics of several silicon carbides. It was in this latter study, that the two silicon nitrides were also examined. Conclusions are reached concerning the elastic nature of the impact resistance and the mechanism of the creep process as well as slow crack growth characteristics and the transient nature of the strength distributions.

INSTRUMENTED CHARPY IMPACT TESTING OF SILICON CARBIDE

A number of commercial silicon carbides were macro-impact tested utilizing an instrumented Charpy type pendulum machine, especially modified for low blow testing.[1] This instrumentation facilitated the separation of the various energy contributions so that it was possible to associate the pertinent features of the oscilloscope load-time traces with various events during the impact process. Figure 1 illustrates the equipment. The energy balance was analyzed by a compliance method and fracture mechanics concepts were applied. Macro- and micro-fractography were performed.

It was concluded that the Charpy type impact test can be used for the energy absorption analysis of the impact resistance of ceramics; however, it is often very difficult to achieve a 100 percent energy balance. An example of the partitioning of the various energy contributions as in Table 1 reveals that most of the energy is contained in the stored elastic strain energies of the machine and the specimen; unfortunately, the machine clearly dominates. The specimen energy is nominally its stored elastic strain energy at fracture. Since most published results of the impact energies of ceramics fail to separate these contributions, it is evident that many early impact studies are reporting data that primarily describes the testing machine rather than the ceramic material. Those early results should be re-evaluated.

Table 2 summarizes the average results for the six SiC materials tested at room temperature. The exact energies are similar to those tabulated in reference 1, with only the energy percentages summarized here. This is because in other studies, the exact amounts of energy absorbed will depend on the specific testing machine and the specimens. Consequently, these energies

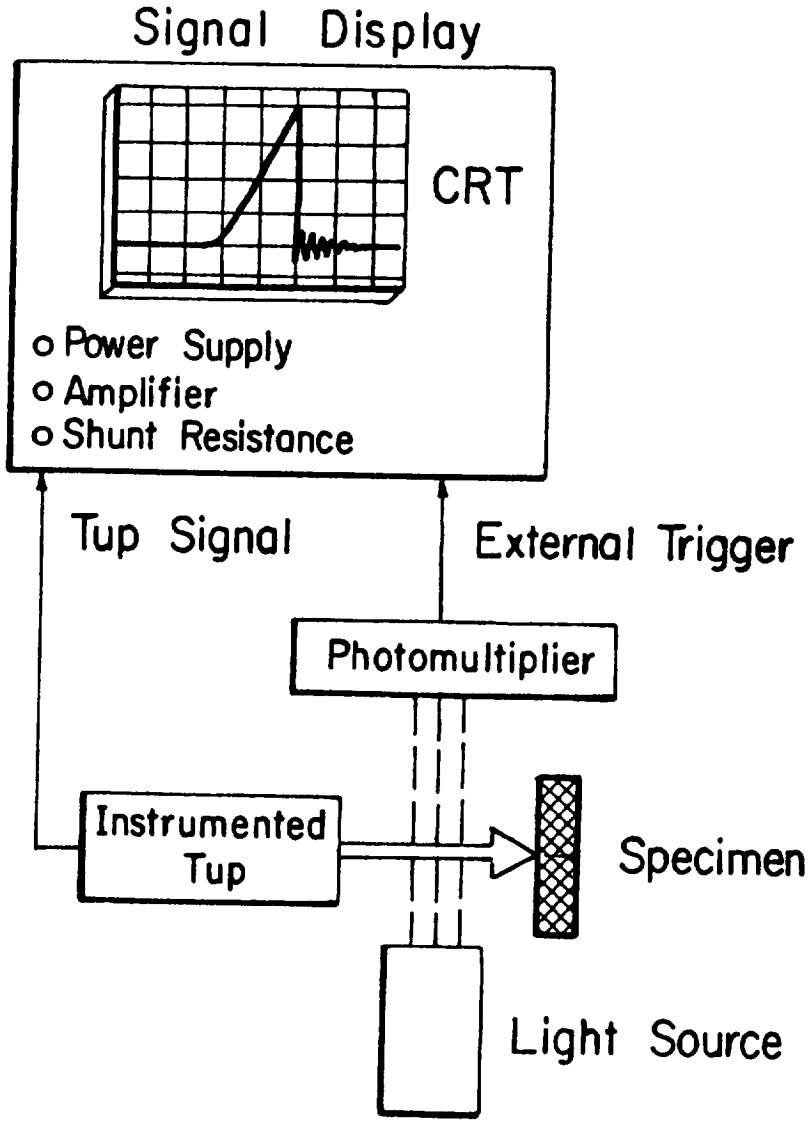

Figure 1. Schematic illustration of the major components for instrumented impact testing

Table 1. Energy Balances for Typical Norton Company NC-400-L Recrystallized Self-bonded SiC Charpy Impact Specimens.

Energy Contributions	SPECIMEN CONDITION: Unnotched (Joules)	Unnotched (%)	Saw-notched (Joules)	Saw-notched (%)	Vee-notched (Joules)	Vee-notched (%)
Stored elastic strain energy in specimen	0.0256	35.7	0.00182	24.7	0.00125	23.6
Stored elastic strain energy in machine	0.0424	59.1	0.00329	44.6	0.00301	56.8
Specimen's vibrational energy[a]	--	< 0.1	--	< 0.1	--	< 0.1
Specimen's kinetic energy before fracture	0.0004	0.6	0.00039	5.3	0.00039	7.4
Specimen's work of fracture[b]	0.0035	4.9	0.00277	37.5	0.00277	52.3
Specimen's kinetic energy after fracture	0.0016	2.2	0.00040	5.4	0.00040	7.6
Sum of above items[b] (Joules) (%)	0.0700	97.6	0.00590	80.1	0.00505	95.4
Total absorbed energy (measured), ΔE_o	0.0718	100.0	0.00738	100.0	0.00530	100.0

[a] The vibrational energies are approximately 10^{-6} Joules.

[b] The work of fractures are not included in the summations. They are in the above table only for a basis of comparison, as it is evident that their energy is derived from the stored elastic strain energy of the specimen and the machine.

or percentages should not be applied to any other form of testing or design; they are applicable only to these tests on this specific Charpy impact machine. They do, however, clearly illustrate the point that more than half of the energy during Charpy impact testing of ceramics is stored in the machine. It varies since the machine compliance is load dependent and thus, also, specimen strength dependent. The energy absorbed by the specimens at failure was simply the stored elastic strain energy at the fracture load in every instance[2].

The instrumented Charpy-type pendulum test can also be utilized for high stressing rate three point bend testing as was demonstrated for a slow crack growth prone soda-lime-silica glass[3] and also for the silicon carbides which are rather strain rate insensitive ceramics at room temperature. For the silicon carbides, the high stressing rate impact results agreed very favorably with those obtained using slow bend tests. The interaction of the specimen strength and compliance to yield high values of absorbed impact energies was demonstrated. The fundamental concepts were extended to quantitatively describe the toughening effects of compliant surface layers on brittle ceramics. It was evident that in order to achieve higher energy absorption using the compliant surface layer approach, ideally, the compliant layers cannot reduce the strength of the substrate ceramic material.

As previously noted, the silicon carbides yielded essentially the same values of fracture toughness for high rates of loading as from slow bend tests. However, fractography revealed a dependence of fracture surface topography on the stored elastic strain energy in the specimen. High strain energy favors rougher fracture surfaces on a macro-scale and transgranular fracture on a micro-scale. There also appears to be a grain size effect superimposed, tending toward intergranular fracture for fine grain sizes. Unfortunately, processing technology for silicon carbide ceramics is not advanced to the state where systematic structural variations are possible, consequently, these general trends could not be further explored on a quantitative basis.

Table 2. Average Energy Partition for Unnotched Charpy Specimens of the Six SiC Materials Tested

Material	% Specimen	% Machine
NC-400L	34.3	58.0
NC-400H	28.7	57.8
KT-SiC	21.3	70.0
SiKa-HP-L	34.0	55.3
SiKa-HP-H	34.7	60.6
NC-203	33.8	55.1

The equipment and techniques previously described for the room temperature low blow Charpy impact testing were modified and extended for elevated temperature impact studies.[4] The equipment modifications were simply ones to permit rapid resistance heating for the silicon carbide specimens while in place on the Charpy testing machine. The impact of 7 commercial and 9 experimental silicon carbide materials were measured in air to 1700°C. The Young's elastic moduli of all of the silicon carbides were also measured using resonance techniques to permit energy absorption calculations. The absorbed impact energy was partitioned into the energy absorbed by the specimen, and by the machine. For the commercial SiC materials tested, it was observed that the fracture stress, the elastic modulus and the impact resistance gradually decreased with increasing temperature. For these SiC materials the temperature dependence of the impact resistance was primarily governed by the decrease of the fracture stress with increasing temperature, since the decrease in the elastic modulus with temperature was relatively small. Table 3 summarizes the results for the Carborundum sintered alpha silicon carbide material while Figures 2 and 3 illustrate the effects of temperature on the impact resistance and the strength of the Carborundum sintered alpha silicon carbide.[5]

All of the commercial SiC materials Charpy impact tested in this study, exhibited purely elastic behaviour to temperatures ≈1600°C. At T's $\geq$ 1600°C, the Carborundum KT-SiC which contains considerable free Si (m.p. 1410°C), did exhibit a propagation-energy type of behaviour where the load-drop from the maximum value was gradual rather then instantaneous as observed for the purely elastic case. The propagation energy type behaviour was also observed for NC-400-L SiC, but at a much higher temperature (1680°C). However, in spite of the occurrence of a propagation energy contribution with increasing temperature, these two SiC materials, the KT and NC-400-L both have rather low fracture stresses and low overall impact resistances at high temperatures.

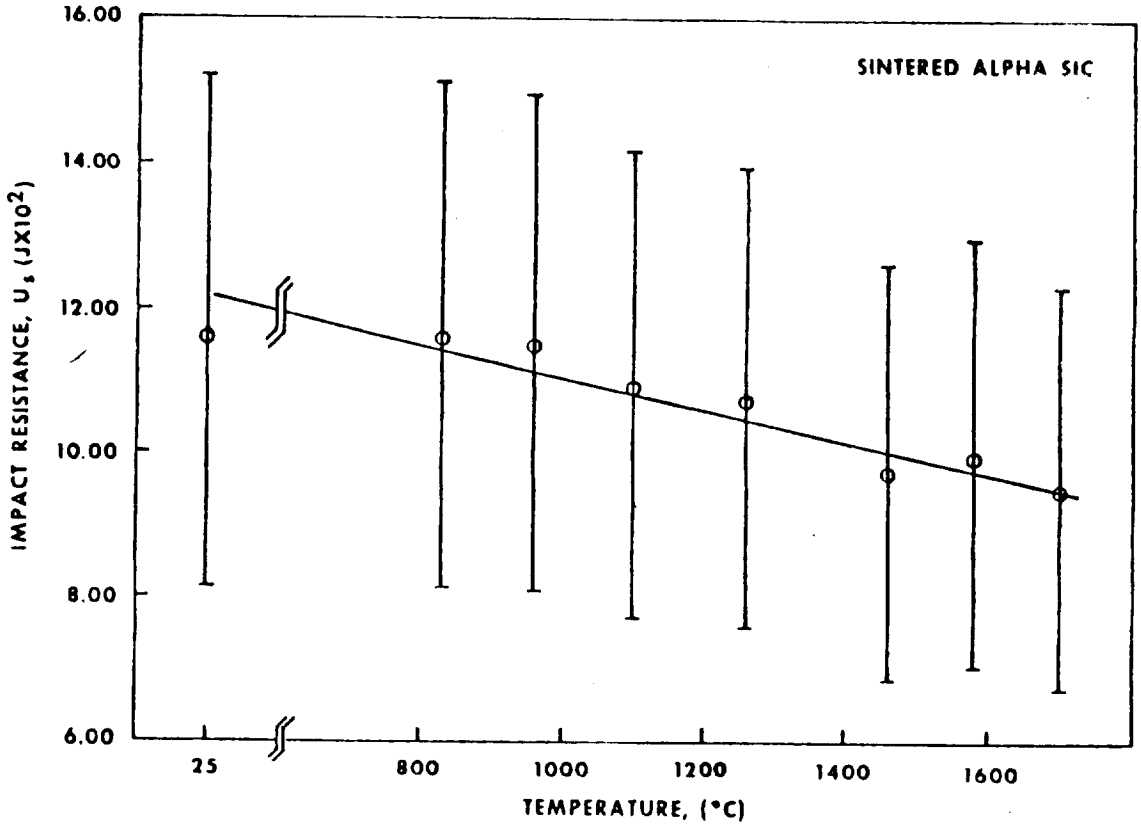

Figure 2. The elevated temperature impact resistance of the Carborundum sintered alpha silicon carbide.

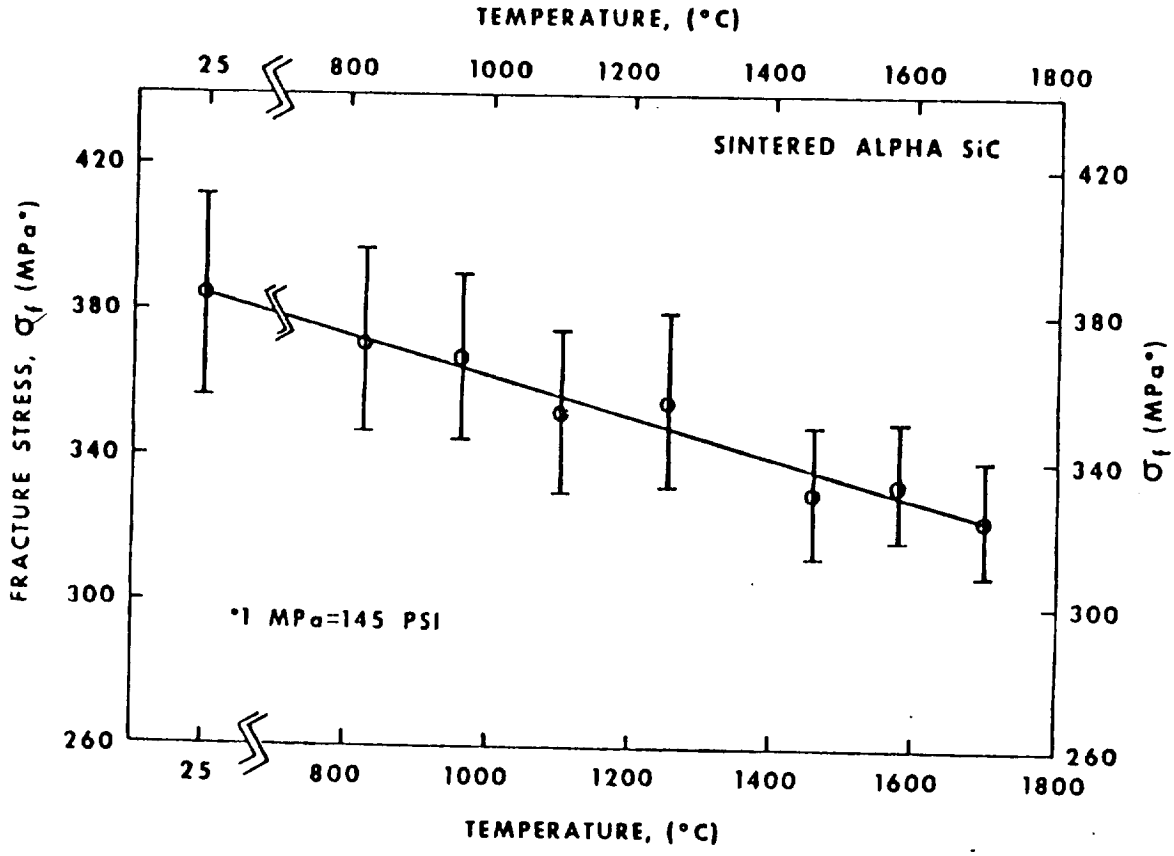

Figure 3. The elevated temperature strengths, impact tested, of the Carborundum sintered alpha silicon carbide.

Table 3. Summary of the Elevated Temperature Charpy Impact Resistance of the Carborundum Company Sintered Alpha Silicon Carbide.

Temperature	Fracture Stress, σ_f (MPa)	Absorbed Impact Energy, ΔE_o ($J \times 10^2$)	Energy Absorbed by The Speciman, U_s ($J \times 10^2$)	Energy Absorbed by The Machine, U_m ($J \times 10^2$)
25	385 ± 28	37.13 ± 10.42	11.67 ± 3.56	20.53 ± 8.58
830	372 ± 25	36.33 ± 9.78	11.58 ± 3.51	20.44 ± 6.01
960	368 ± 23	36.70 ± 10.10	11.51 ± 3.44	19.92 ± 5.94
1100	353 ± 22	34.74 ± 10.02	10.94 ± 3.22	18.42 ± 5.26
1260	356 ± 24	30.50 ± 8.74	10.76 ± 3.17	18.73 ± 5.51
1460	331 ± 18	33.12 ± 9.64	9.75 ± 2.87	16.21 ± 4.76
1580	334 ± 16	31.35 ± 8.96	9.99 ± 2.94	16.50 ± 4.85
1700	324 ± 16	29.27 ± 8.74	9.53 ± 2.80	15.52 ± 4.56

A series of special experimental silicon carbide microstructures were also prepared in this study. Two types were consolidated, one to possess a duplex grain size distribution or microstructure, the other a series to contain a fibrous grain morphology. The objective was to create microstructural inpediments to crack growth during the fracture process. Figure 4 illustrates the fine grain size matrix material, while Figure 5 contains a micrograph of the coarse CVD grain material. Figure 6 depicts the material with fibers added. Duplex microstructures were consolidated to contain 20% of coarse CVD grains, while fibers were successfully added to a 10% level. Larger additions of fibers did not densify during the hot pressing consolidation.

The results of these designed microstructures containing coarse secondary grains and also those with fiber additions were disappointing. The room temperature impact fracture stresses and the elastic moduli decreased with increasing amounts of the coarse CVD grains and the fibers, respectively. These decreases were more pronounced for the fiber additions than for the coarse grain additions. The additions apparently served as fracture origins as well as inhibiting densification during processing, thus neither the coarse grains nor the fibers enhanced the impact resistance.

All of the experimental SiC Materials tested in this study exhibited purely elastic behavior to about 1600°C. The temperature dependence of the fracture stress, the elastic modulus and the impact resistance for the experimental SiC materials indicated a gradual and monotonic decrease with increasing temperature, similar to the commercial SiC materials. Also, the temperature dependence of the impact resistance was primarily governed by the decrease of the fracture stress with increasing temperature;

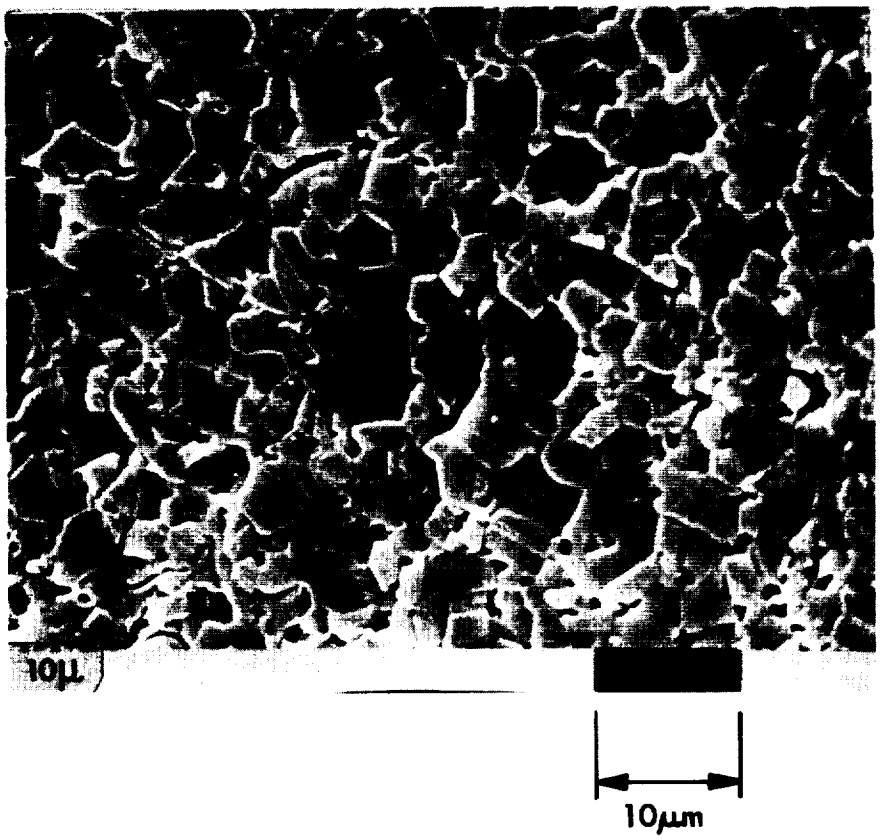

FIGURE 4

The microstructure of the hot pressed, SIKA-HP SiC without any fibrous or large CVD grains added. This sample was polished, etched chemically with (90% KOH, 10% KNO_3) at 525°C in a Ni-crucible. The average grain size is about 7 µm and relatively equiaxed. Although the material is nearly theoretically dense, the etching accentuates small pores yielding the appearance of a large pore-like structure at many of the triple points.

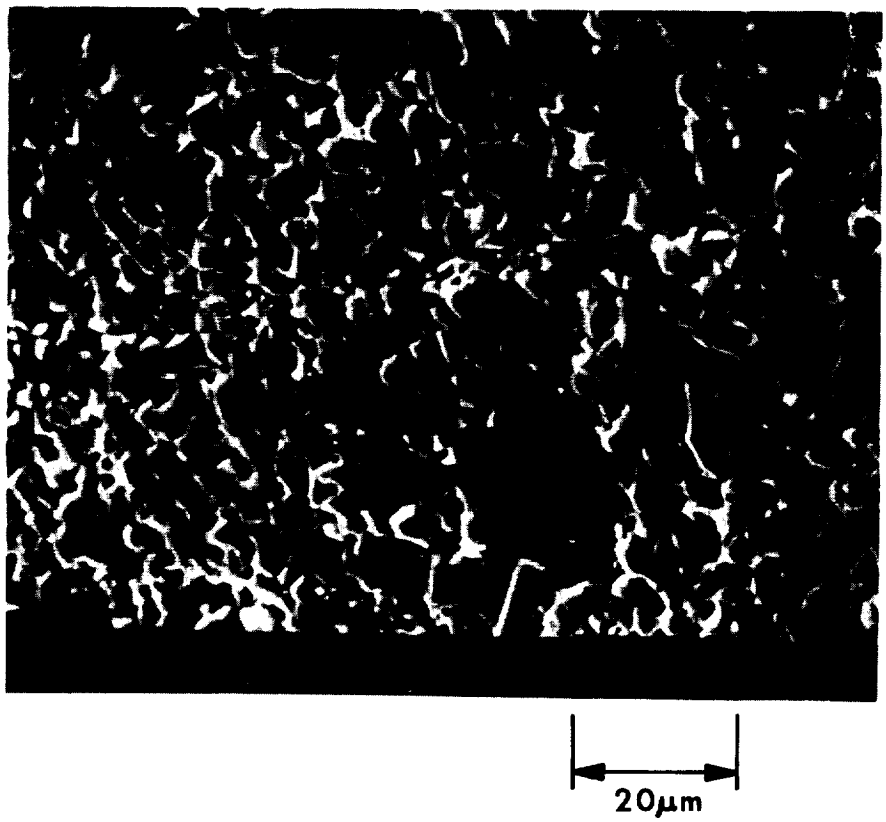

FIGURE 5

The microstructure of the hot pressed experimental SIKA-HP-5 CVD SiC. The sample was polished, etched chemically as in Fig. 22 and examined with the SEM. The continuous matrix of fine grains contains large CVD SiC grains (5 wt %). These CVD SiC grains are considerably larger than the matrix grains. A small amount of intragranular porosity can be seen within the large CVD grains.

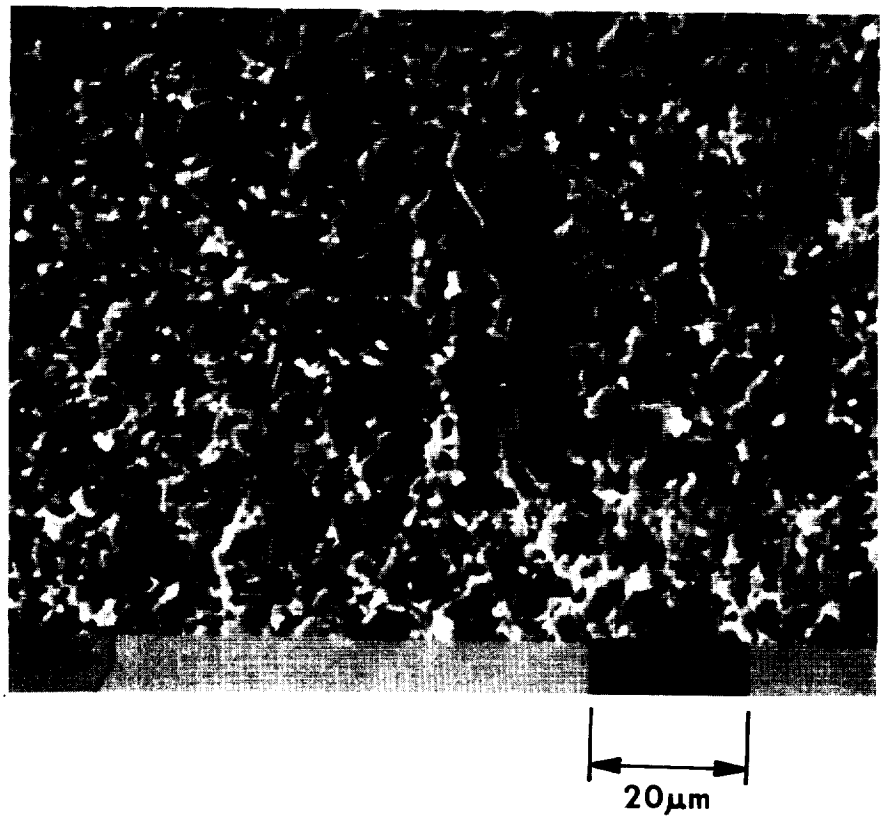

FIGURE 6

The microstructure of the hot pressed experimental SIKA-HP-5 F1B SiC. The sample was polished, chemically etched (as in Figure 22) and examined with the SEM. The matrix is fine grained and the fibrous grains are 20-30 μm long and about 4 μm wide. There is a small amount (~1%) of porosity located predominantly at grain boundaries.

however, the elastic modulus also decreased, but only a small amount. The elevated temperature impact resistance was not enhanced significantly by the grain or the fiber additions to the microstructures.

In a purely practical sense, it is apparent that the polycrystalline silicon carbide commercially available today, does not exhibit any substantial ductility during fracture below about 1650°C. Its impact resistance, in terms of the energy absorption is derived almost totally from its fracture stress and the stored elastic strain energy at fracture.[4,5]

STRENGTH DISTRIBUTIONS OF SILICON CARBIDES AND NITRIDES - OXIDATION EFFECTS

As-machined strength distributions were examined for two commercially available silicon carbides, Carborundum's sintered alpha silicon carbide[6] and Norton's hot-pressed NC-203. A two parameter Weibull analysis was performed and revealed that multiple (concurrent) flaw populations were present, consisting of edge flaws and also surface flaws on the machined surface. The sintered alpha silicon carbide had a Weibull modulus of 6.7 and exhibited a greater than 97% fit to a single two-parameter Weibull expression in spite of the presence of at least two obvious flaw populations as previously noted. The hot-pressed NC-203 had a slightly higher Weibull modulus of 8.9, indicating a narrower distribution. These two Weibull moduli are typical of those for most silicon-ceramics, they reflect a combination of the intrinsic material properties, the sample preparation by machining, and probably also the testing procedure itself.

In addition to the two silicon carbide materials, two commercial silicon nitride materials were also studied in a similar manner.[7] The Wesgo sintered SNW-1000 also followed a Weibull expression for the as-machined condition and had a correlation coefficient of greater than 95% with a Weibull modulus of 8.2. The Norton NCX-34 was an experimental silicon nitride material fabricated by hot pressing. Its as-machined strength distribution exhibited a wide low strength tail which disappeared during high temperature oxidation. Nevertheless, even with the low strength flaws present, a Weibull modulus of 4.4 and a correlation coefficient of 79% was determined.

Once the as-machined strength distributions of these two silicon carbides and two silicon nitrides were determined, the effects of oxidation and oxidation under load were determined.[7-9] The results are encouraging in that strengthening

and increases of the Weibull modulus may be effected by oxidation; however, the transient nature of the flaw populations presents a very complicated situation.

The effects of oxidation at 1370°C in air for several different exposure times varied for each material. Results for the Carborundum sintered alpha silicon carbide are shown in Figure 7. The strength distribution of this material exhibited little change, even after oxidation for 50 hours. Although the Weibull modulus increased from 6.7 to 11.0, the average strength never varied more than 25 MPa from that of the as-machined specimens. Since the strengths of these specimens are controlled primarily by surface flaws, it is evident that the oxidation did not significantly change those flaws in this material. The correlation coefficients for the distributions after oxidation are all greater than 92%, indicating that the two-parameter Weibull expression still fits the data satisfactorily.

The hot-pressed NC-203 silicon carbide exhibited increased strengths after short 1370°C oxidation periods of up to one hour. The changes are shown in Figure 8. The increased strengths are due to "healing" of the machining flaws by the formation of the oxide film, which may blunt the flaw tips, making them less severe stress concentrators. Longer exposure times resulted in the formation of bubbles and pits on the oxidized surfaces, which eventually superceded the machining damage as the strength controlling flaws. These defects decreased the strength. The Weibull modulus exhibited a significant increase, from 8.9 (as-machined) to 30.9 after oxidation for 50 hours, indicating that the distribution of the flaws responsible for failure becomes much more uniform after oxidation. This is in contrast to Carborundum's sintered alpha silicon carbide material, where the average strength showed little change, and the width of the strength distribution also remained relatively constant. The correlation coefficients of greater than 90% indicate a good fit to the two-parameter Weibull expression.

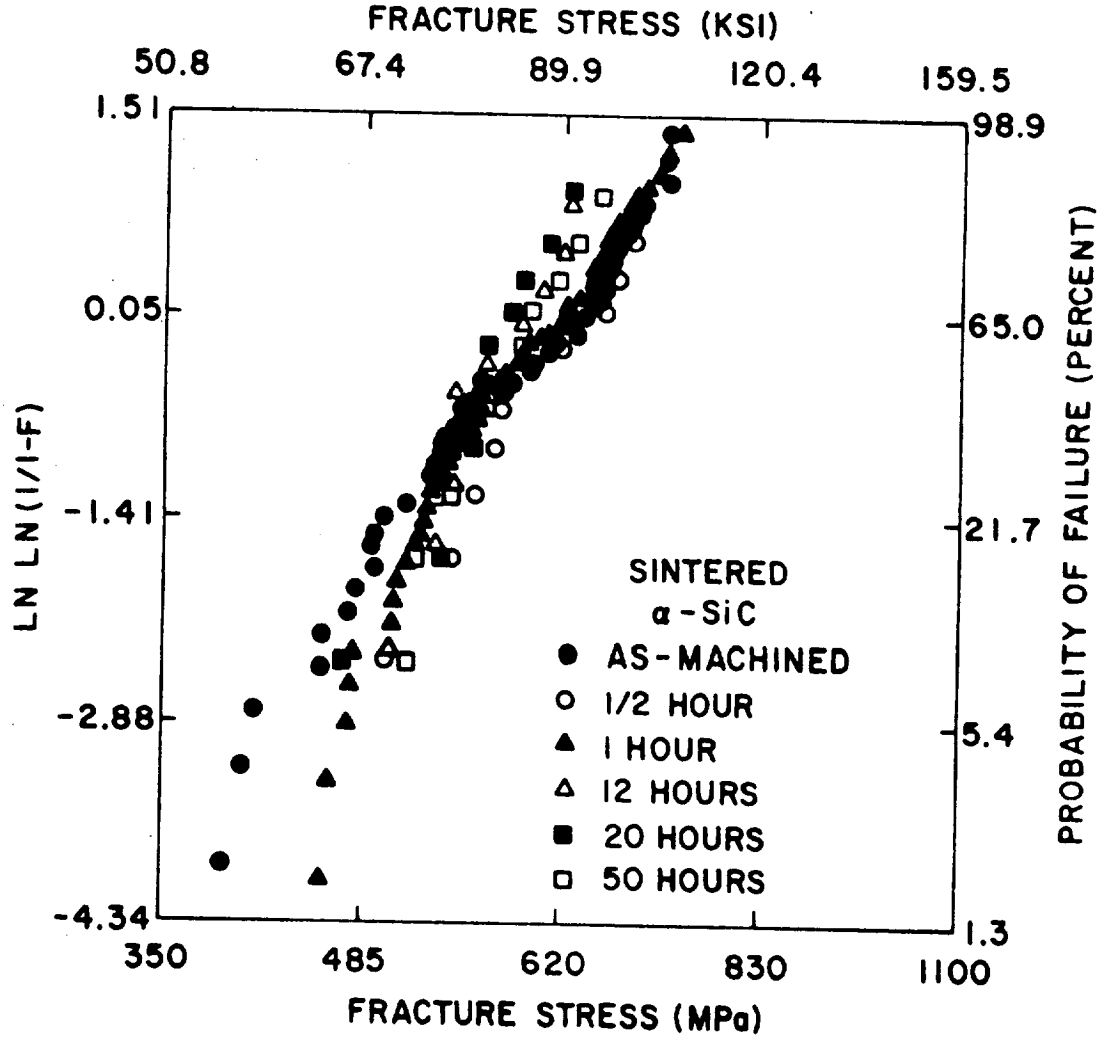

Figure 7. The strength distributions of sintered alpha silicon carbide as affected by oxidation in air at 1370°C.

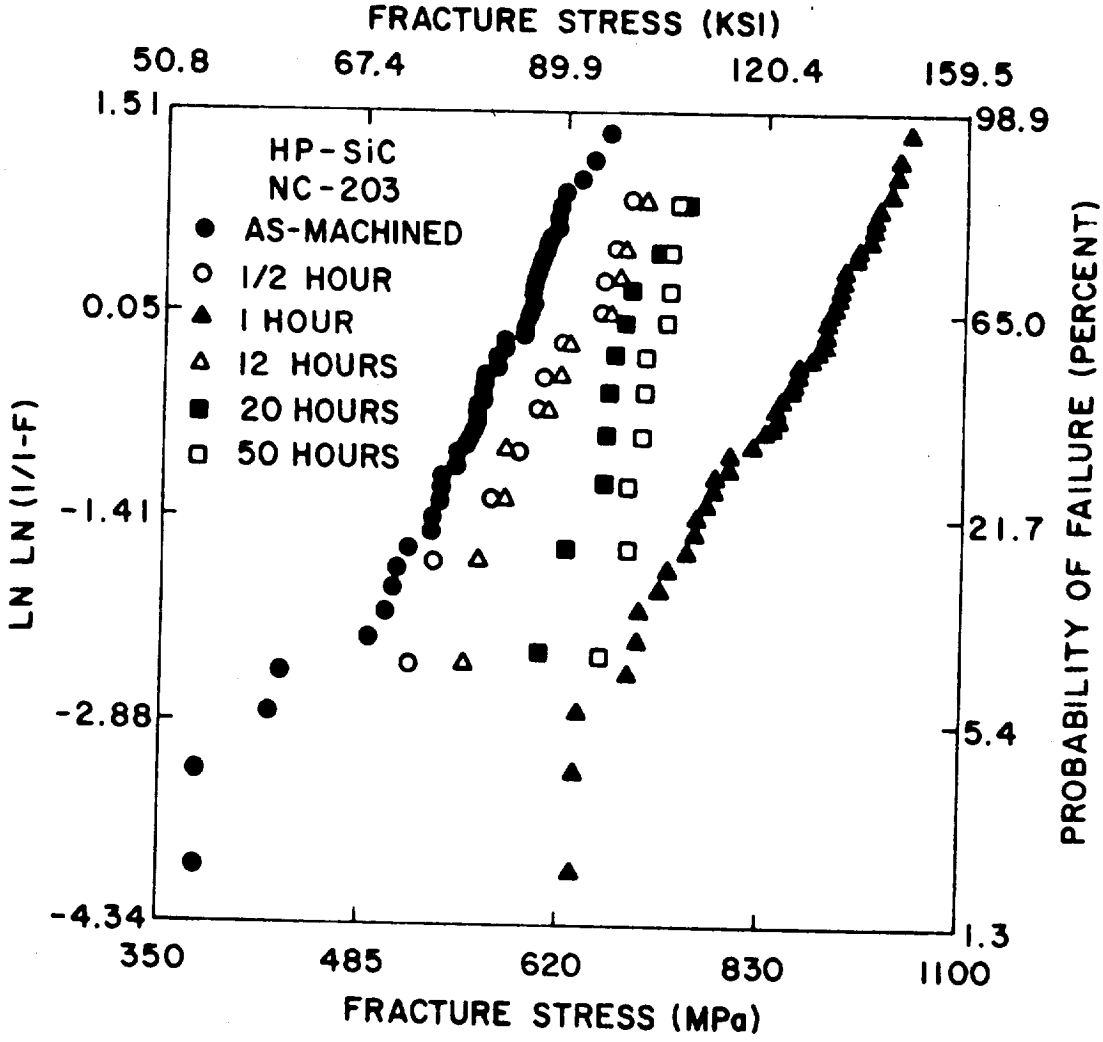

Figure 8. The strength distributions of the hot-pressed NC-203 as affected by oxidation in air at 1370°C. Note the strength increases and compare with Figure 4.

Oxidation at 1370°C of the sintered SNW-1000 silicon nitride proved to be detrimental to the room temperature strength of the material. Except for the one-half hour oxidation period, which resulted in a slight increase in strength, a continuous loss in strength was observed and is shown in Figure 9. This is related to the alteration of the specimen surfaces by oxidation, especially to the creation of a very irregular oxide/nitride interface. Since the flaws are increasing in severity, it's not very consoling that the improvement in the Weibull modulus indicates that the flaws are also becoming much more uniform.

As for the other materials, these strength distributions are also very well described by a two-parameter Weibull expression. Oxidation also consistently resulted in strength reductions for the hot-pressed NCX-34 silicon nitride material as shown in Figure 10. The removal of the wide low-strength tail observed in the as-received distribution resulted in a significant increase in the Weibull modulus, from 4.4 to 14.0 (oxidized for one hour). As for the sintered silicon nitride, the creation of more severe flaws during oxidation resulted in the strength reductions. Except for the as-machined strength distribution, the correlation coefficients again were greater than 90%.

In some cases during oxidation under an applied load, competitive processes between two types of flaw behavior were observed. These phenomena include the processes of flaw "growth" and flaw-tip "blunting". The interaction between these two processes was found to be very complex, and not completely explained by the present study. The sintered alpha-silicon carbide experienced a decrease in strength of about 80 MPa after application of the lower applied load, as compared to the strength after a similar oxidation without any applied load. As shown in Figure 11, the entire distribution shifted to lower strengths, but still exhibited a greater than 98% fit to the two-parameter Weibull expression.

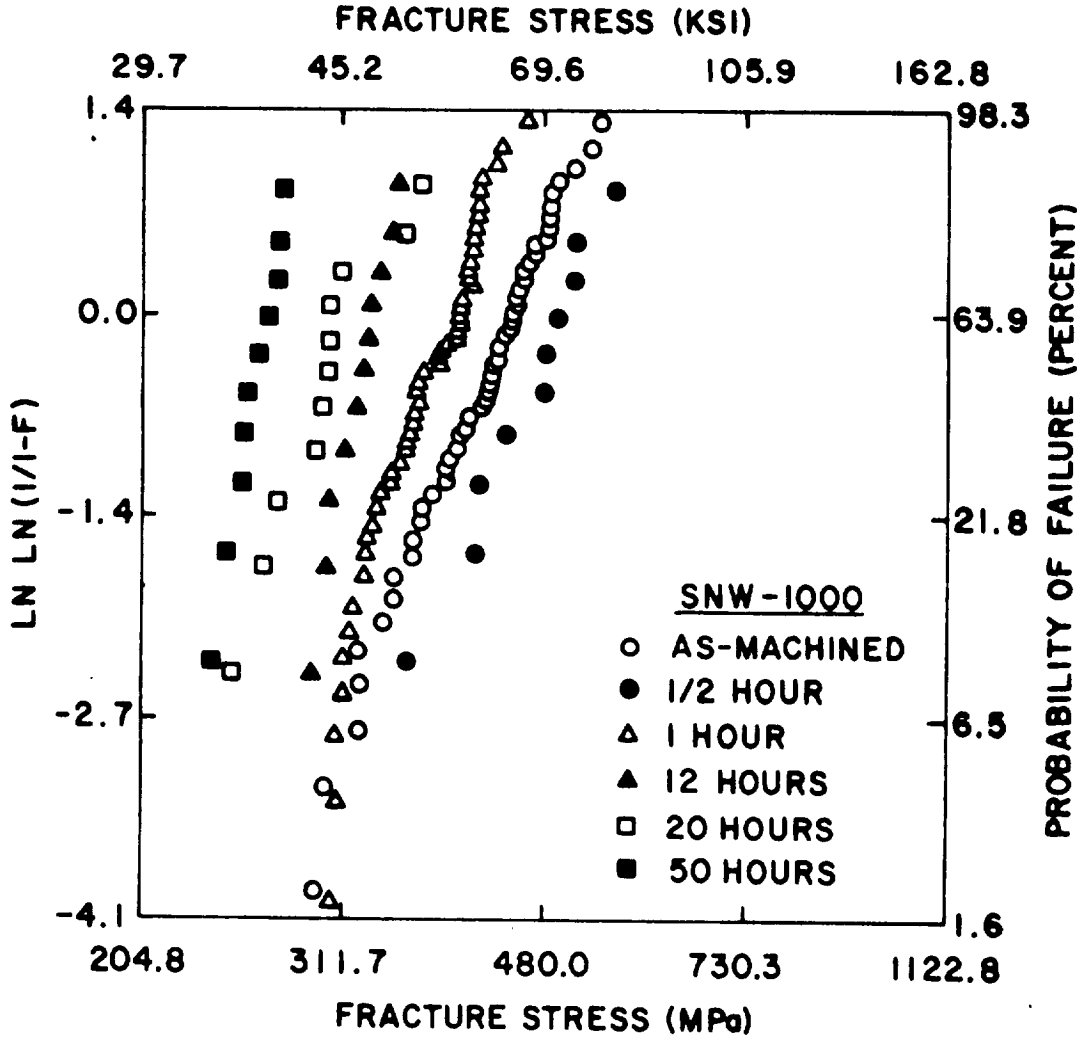

Figure 9 Effects of oxidation at 1370°C in air on the strength distributions of the sintered SNW-1000 silicon nitride. Compare with Figures 4 and 5 and note strength decreases in contrast to the increases for the silicon carbides.

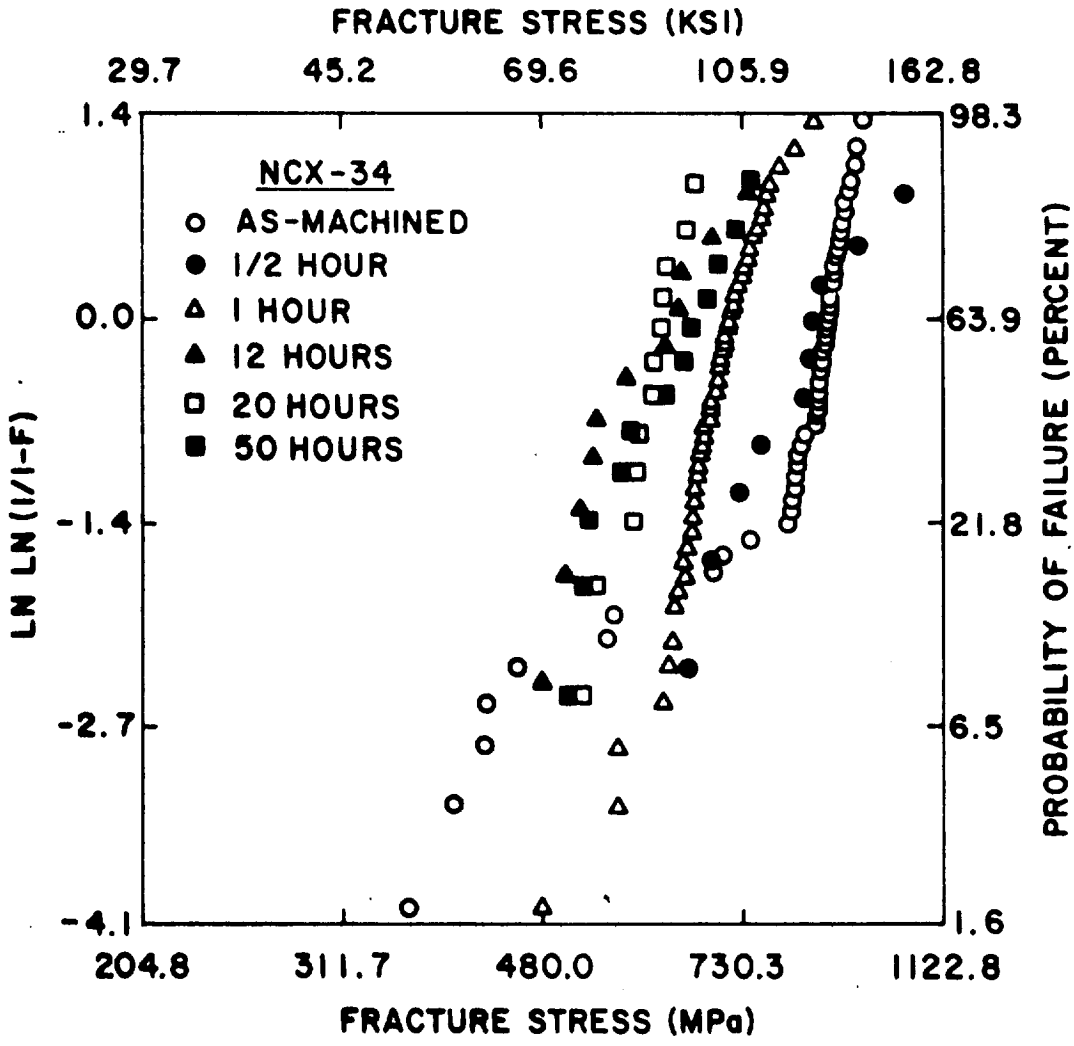

Figure 10. Effects of oxidation in air at 1370°C on the strength distributions of the hot-pressed NCX-34 silicon nitride.

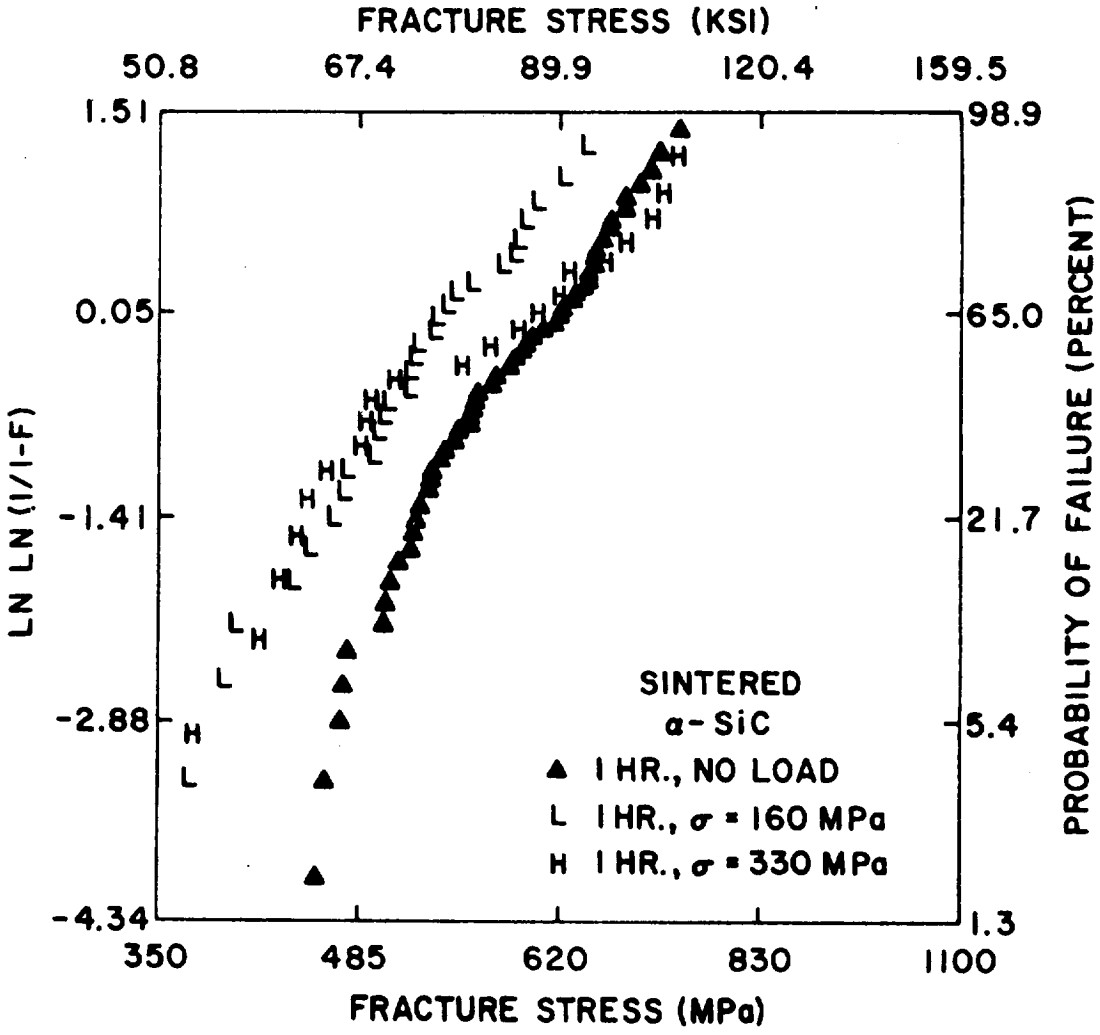

Figure 11. The effects of applied loads during oxidation on the strength distributions of the Carborundum sintered alpha silicon carbide. Note that the higher applied stress crosses over the original distribution indicating a K_{Ith}, a threshold stress intensity.

The behavior can be tentatively explained in terms of a crack growth process which is activated by the applied stress. Application of the higher applied load, however, does not result in the intuitively expected enhanced flaw growth. Rather, there is a transition in the distribution to higher strengths, which prevails in the high strength (small flaw size) regime. This behavior indicates that a flaw tip "blunting" process is at first (low strength regime) in competition with the flaw growth process, and eventually dominates over the flaw growth process (high strength regime). The results indicate that this is dependent on the flaw size; a critical size is necessary before flaw growth will occur. It is illuminating to consider this observation in terms of the stress intensity. It suggests the existence of a threshold stress intensity, K_{Ith}, below which crack healing or blunting may occur and above which growth occurs. If indeed such a K_{Ith} exists, it may be extremely important for design purposes as it possesses some analogy to a fatigue limit, K_{Io}.

The behavior of the Norton hot-pressed NC-203 silicon carbide is very similar to that of the Carborundum sintered alpha silicon carbide material with regard to the oxidation-under-load experiments as shown in Figure 12. The lower static load results in reduced strengths for the entire distribution, except at the high strength tail. The observed transition is analogous to that seen for the sintered material for the case of the higher applied load where flaw growth is seen to have a decreasing effect at the smaller flaw size high probability of failure levels. Application of the higher load for the hot-pressed silicon carbide resulted in no change in the strength distribution, as compared to that for oxidation without any load. Since the lower load resulted in flaw growth, it appears that the higher load suppresses this stage and advances to the flaw blunting previously noted. Again, these complex flaw growth, flaw blunting interactions cannot be fully described within the scope of the present study.

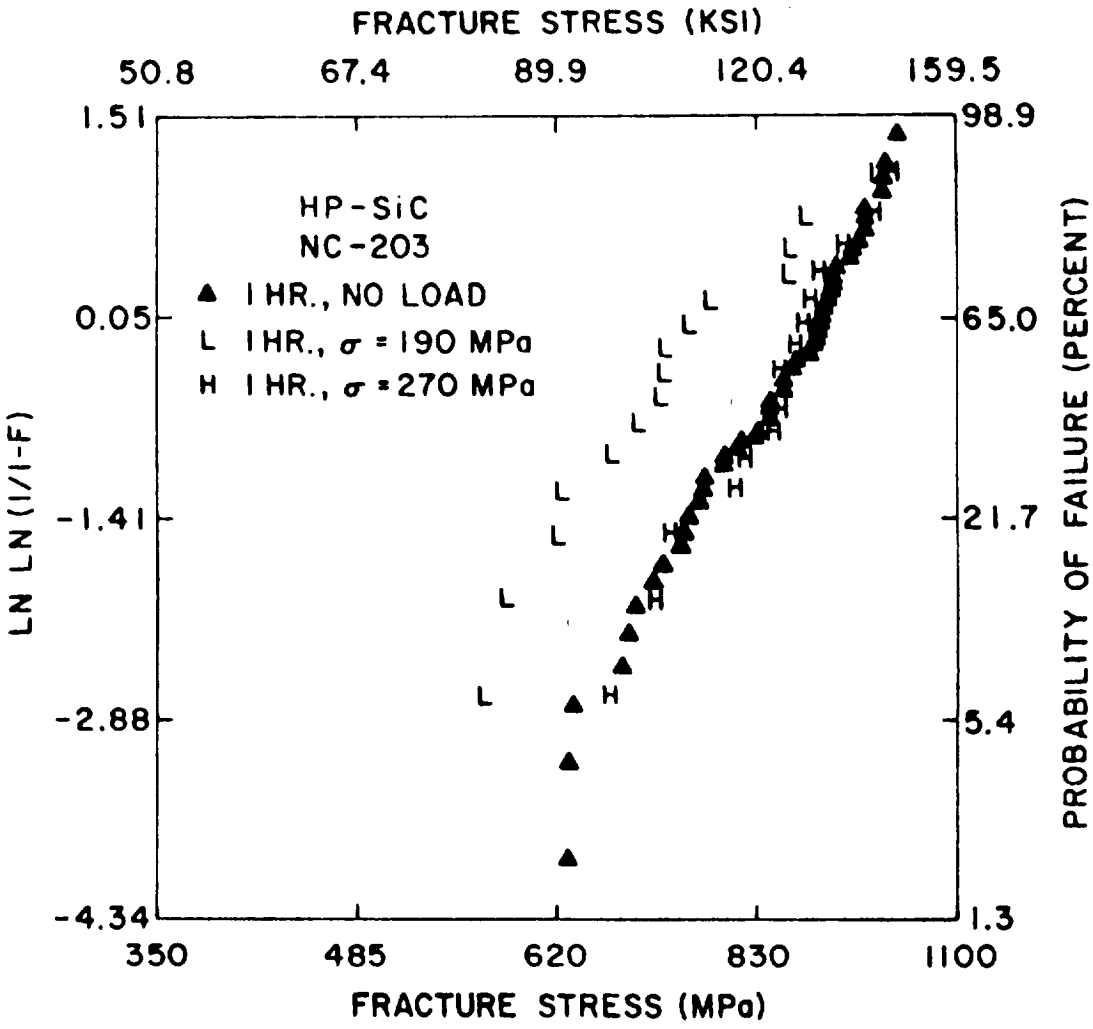

Figure 12. The effects of applied loads during oxidation on the strength distributions of the Norton hot-pressed NC-203 silicon carbide.

For the sintered SNW-1000 silicon nitride, oxidation under both the high and low static loads resulted in increased strengths as shown in Figure 13. The lower applied load resulted in the highest strengths. This behavior may be described in terms of a "blunting" process which occurs by grain boundary sliding at the crack tip. In addition, a compressive stress may possibly be quenched-in at the crack tip upon unloading. The combination of "blunted" flaw tips and the beneficial residual stress may account for the increased strengths. The higher applied load resulted in a smaller degree of strength improvement. This case may be interpreted that the flaws extended a limited amount in combination with the blunting process. The increased flaw lengths shift this distribution to the left of that which experienced the lower applied load. The competing flaw-tip blunting and flaw growth phenomena are again observed for this material. It is interesting to speculate that if an extended systematic series of different stress levels were experimentally investigated a K_{Ith} may be observed in this sintered silicon nitride. The behavior of the hot-pressed NCX-34 Si_3N_4 can be reasonably described by a straight-forward flaw growth process. Successively higher loads during oxidation resulted in correspondingly lower strengths, as shown in Figure 14. This indicates that the applied load causes a proportional amount of crack growth.

In general, it was observed that at least two processes actively control the strength behavior of silicon ceramics after oxidation under an applied load. These processes appear to be in competition. A flaw blunting process may occur, perhaps by grain boundary sliding at the flaw tip under the tensile stress field. In other cases, flaw growth by grain boundary separation may predominate. The parameters influencing which of these processes will dominate in any particular situation may include the flaw size and its associated stress intensity factor, and the orientation of the grains at the tip of the flaw with respect to the crack propagation direction. Also, the conditions at the

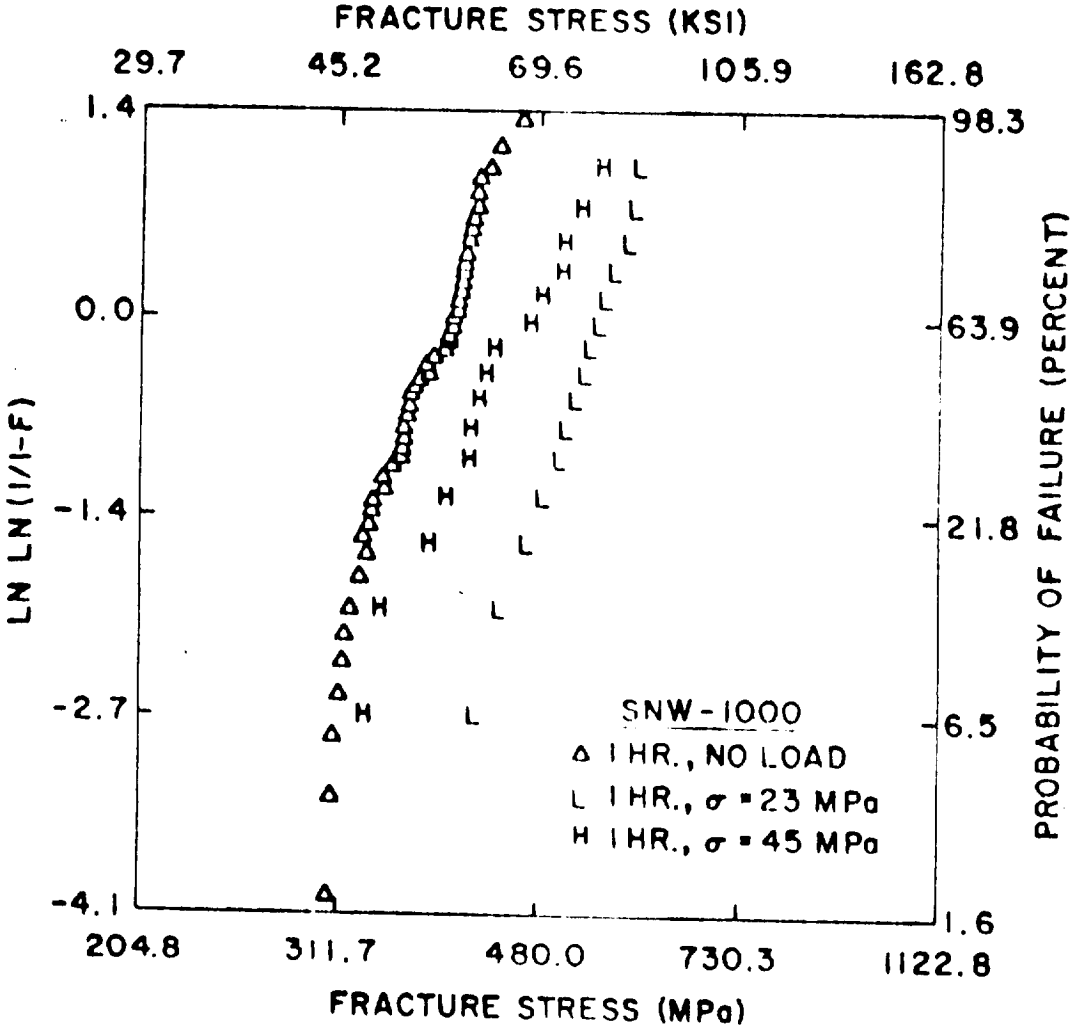

Figure 13. The effect of oxidation under load on the strength distributions of SNW-1000. Note the strengthening effect of the loads.

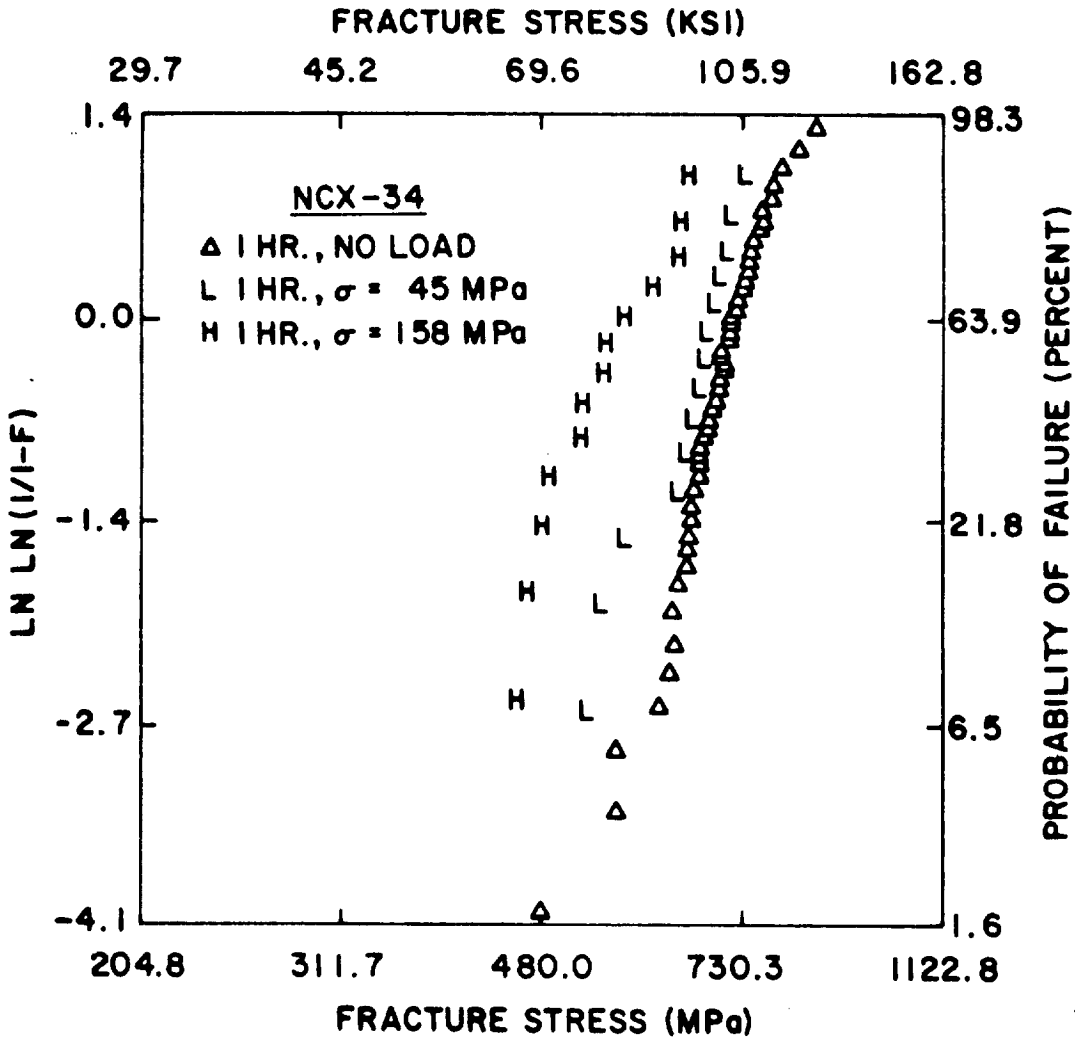

Figure 14. The strength distributions of hot-pressed NCX-34 Si_3N_4 after oxidation under static load for one hour at 1370°C. Compare with Figure 10.

grain boundaries, especially with respect to second phases introduced as sintering and hot-pressing additives, and their state (glassy, crystalline) after oxidation, are important. The transient conditions during the static loading experiments, such as simultaneous oxidation, may in themselves add to the complexity of the interactions between the above two phenomena.

Several important aspects of the strength distributions of silicon ceramics during oxidation and oxidation-under-load have been revealed. It is obvious that the strength distributions, although often describable by a single Weibull function are, in fact, a combination of several different flaw distributions. A serious concern in this respect is that scaling of results may prove non-conservative if the geometry of the test samples and real engineering parts are not identical, that is the edges, surfaces, corners, etc. scale appropriately. The other obvious point is that the flaw distributions at elevated temperatures under load are highly transient in nature. These distributions often cannot be described by the Weibull distribution and appear to be extremely complex. These flaw distributions and their transient characteristics are probably material and environment specific.

DYNAMIC FATIGUE OF OXIDIZED SILICON CARBIDES AT ELEVATED TEMPERATURES

Nine different commercial silicon carbide materials manufactured by the processing techniques described below, were examined for their slow crack growth resistance between 1000°C and 1400°C.[10,11] Selected room temperature properties of these silicon carbides are summarized in Table 4. From the empirical crack growth law:

$$V = A\left(\frac{K_I}{K_{Ic}}\right)^N$$

it has been shown that the stressing rate dependence of strength can be expressed as:

$$\sigma_f = B\,\dot{\sigma}^{\left(\frac{1}{N+1}\right)}$$

where the N-value is a measure of the material's resistance to slow crack growth. Measuring the fracture stress, σ_f, as a function of the stressing rate, $\dot{\sigma}$, enables an estimate of the N-parameter from the slope of the log σ_f vs. log $\dot{\sigma}$ graph. This dynamic fatigue, stressing rate technique was used and correlated with methods of processing, chemistry, and microstructural characteristics of the silicon carbides listed in Table 4. The results are summarized in Table 5. Conclusions that can be drawn are that definite trends exist in the N-parameters for the slow crack of silicon carbides with respect to the method of processing the materials.

$$N_{\substack{\text{hot-pressed}\\ \text{SiC}}} < N_{\substack{\text{sintered}\\ \text{SiC}}} < N_{\substack{\text{free-Si}\\ \text{containing SiC}}}$$

The most susceptible silicon carbide materials to slow crack growth are the hot-pressed materials. Below 900°C, these materials have all been reported to have good resistance to slow crack growth with N values reported between 80 and 100. However, above 1000°C, the materials containing sintering aids, including the Norton hot-pressed NC-203 and the Carborundum sintered alpha silicon carbide, have much lower N values (20 to 70), which suggest that the

TABLE 4: SELECTED ROOM TEMPERATURE MECHANICAL PROPERTIES OF THE SILICON CARBIDES

Materials	ρ(gm/cm^3)	G.S.(μm)	E(GPa)	G(GPa)	ν	MOR(MPa)	K_{Ic} (MPa m$^{1/2}$)
Sint-α-SiC	3.15	7	410	180	0.14	425	3.94 $\pm$ 0.20
NC-400-L	2.70	<10,140	256	107	0.20	148	1.18 + 0.15
NC-400-H	2.75	200	250	103	0.21	105	1.73 $\pm$ 0.13
β-HP-SiC	3.17	20-30	440	185	0.18	265	3.84 $\pm$ 0.19
NC-201-HP	3.32	1-5	440	189	0.17	728	3.95 $\pm$ 0.20
NC-203-HP	3.35	1-5	442	185	0.19	760	3.97 + 0.26
KT-SiC	3.10	130	374	156	0.20	147	2.37 $\pm$ 0.18
NC-430	3.09	<10,170	380	155	0.23	117	1.91 + 0.16
NC-433	3.05	<10,100	355	148	0.20	105	1.72 $\pm$ 0.29

TABLE 5: MEASURED N-VALUES OF THE SILICON CARBIDES

Temperature	Sint-α-SiC	NC-400-L	NC-400-H
1000°C	61 ± 7	124 ± 17	130 ± 21
1100°C	55 ± 9	110 ± 15	132 ± 9
1200°C	62 ± 9	116 ± 20	99 ± 7
1300°C	70 ± 10	105 ± 21	110 ± 14
1400°C	55 ± 11	90 + 16	104 ± 31
Temperature	**β-HP-SiC**	**NC-201-HP**	**NC-203-HP**
1000°C	28 ± 5	29 ± 5	30 ± 5
1100°C	---	49 ± 9	43 ± 9
1200°C	21 ± 8	49 ± 11	25 ± 7
1300°C	---	55 ± 8	22 ± 4
1400°C	30 ± 6	67 ± 7	23 ± 5
Temperature	**KT-SiC**	**NC-430**	**NC-433**
1000°C	195 ± 27	135 ± 14	153 ± 26
1100°C	162 ± 24	150 ± 19	140 ± 15
1200°C	153 ± 19	152 ± 22	142 ± 19
1300°C	166 ± 21	142 ± 16	124 ± 22
1400°C	250 ± 37	124 ± 17	110 ± 21

hot-pressing and sintering aids are responsible for a decrease in the resistance to slow crack growth at these elevated temperatures.

Although not hot-pressed, the Carborundum sintered alpha silicon carbide has a relatively low N value, probably due to the detrimental effects of the sintering aids on slow crack growth between 1000°C and 1400°C. The Norton recrystallized self-bonded sintered varieties of silicon exceed 100 at temperatures of 1400°C and below. Free silicon-containing reaction bonded materials are very resistant to slow crack growth throughout the entire temperature range studied, with N values exceeding 100 in all cases. Crack "blunting" caused by the viscous flow of free silicon may have been responsible for these silicon carbide materials superior resistance to slow crack growth.

In general, a trend of decreasing N values was observed with increasing temperature, except in the case of the hot-pressed NC-201 silicon carbide, where the reverse trend occurred. In some of the silicon carbide materials with very high N values a vacillating trend of N values occurred, as for the KT-SiC material. This was due in part to the miniscule difference in slope of the ($\log \sigma_f / \log \dot{\sigma}$) plots at these very high N values, and partially to the errors in the estimating technique used in determining N values. Dynamic fatigue is a difficult method for analyzing slow crack growth when strengths are low and the N values are high, for the critical flaw size is much larger than the extent of flaw growth during the test, particularly for the high N materials.

The commercial SiC materials with lower strengths, such as the free silicon-containing and recrystallized, self-bonded, sintered varieties have relatively high resistance to slow crack growth as they possess high N values. The higher strength fine grained materials containing sintering aids had relatively little resistance to slow crack growth above 1000°C. Table 6, which is a general

summary of silicon carbide N-values confirms this trend by a number of other investigators. The N values decrease above 1000°C.

Although these SiC bodies clearly illustrate that the resistance to slow crack growth is chemistry and microstructure specific, a general axiom may be apparent. In these bodies, the presence of densification aids, whether for hot-pressing or for sintering, generally decreases the material's resistance to slow crack growth.

TABLE 6: SUMMARY OF PUBLISHED SLOW CRACK GROWTH N-VALUES FOR SILICON CARBIDES

Primary Author	Type of SiC	N-Value	Temperature	Atmosphere	Test Type
MCHENRY(23)	NC 203 HP	187	RT	Air	Double Torsion
LANGE(15)	Hot Pressed	80	RT	Water	Double Torsion
MCHENRY(13)	NC 203 HP	100	RT	Water Vapor	Double Torsion
MCHENRY(13)	NC 203 HP	110	600°C	Air	Double Torsion
LANGE(15)	Hot Pressed	>200	600°C	Air	Double Torsion
MCHENRY(16)	NC 203 HP	20	900-1100°C	10^{-4}-10^{-8} P_{O_2}	Double Torsion
HENSHALL(17)	NC 203 HP	40	1000°C	Air	Delayed Fracture
MOUSSA(18)	α-SiC-HP	30	1000°C	Vacuum	Dynamic Fatigue
HENSHALL(19)	NC 203 HP	40	1000°C	Air	Delayed Fracture
HENSHALL(17)	NC 203 HP	25	1100°C	Air	Delayed Fracture
QUINN(6)	B-sintered	41	1200°C	Air	Delayed Fracture
HAMANO(22)	SC-201	33	1200°C	Air	Double Torsion
HENSHALL(17)	NC 203 HP	16	1300°C	Air	Delayed Fracture
MOUSSA(18)	α-SiC-HP	19	1300°C	Vacuum	Dynamic Fatigue
GRELLNER(12)	Al-sintered	10	1370°C	---	Dynamic Fatigue
GRELLNER(12)	Al-sintered	18	1370°C	---	Dynamic Fatigue
LANGE(15)	Hot-Pressed	20	1400°C	Air	Double Torsion
MINFORD(21)	NC 203 HP	20	1400°C	-10^{-10} P_{O_2}	Dynamic Fatigue
HAMANO(22)	SC-201	15	1400°C	Air	Double Torsion
TRANTINA(14)	B-sintered	50	1500°C	Air	D.Tor./Dyn.Fat.
HENSHALL(19)	NC 203 HP	7	1500°C	Air	Delayed Fracture

Note: The numbers following the authors can be traced to their original papers through reference (11) of this report.

FLEXURAL CREEP OF SILICON CARBIDES

The creep rates of four silicon carbide materials, three commerical and an experimental hot-pressed one were measured in air between 1450°C and 1575°C at stresses between 34.5 MPa (5,000 psi) and 172.4 MPa (25,000 psi). These high temperatures and stresses were necessary to obtain measurable and reproducible creep rates. Specimens approximately 1 mm x 1 mm x 300 mm, were tested in three-point bending. By measurements at different stresses and temperatures, for strains below 5%, the stress exponents and activation energies were estimated from the steady state creep rates. Figures 15 and 16 illustrate the results, which are summarized in Table 7 for comparison. In general these creep rates are rather low. At 69 MPa (10,000 psi), the activation energies between 1450°C and 1575°C ranged from 140 Kcal/mol for the hot-pressed Carborundum SiKa-HPL, an experimental material, and 144 Kcal/mol for Norton's NC-400L, to 231 Kcal/mol and 237 Kcal/mol for the Carborundum sintered α-SiC and the Norton hot-pressed NC-203 respectively. These are rather high activation energies for many activated processes. The stress exponents between 1 and 2 are suggestive of grain boundary flow processes, rather than lattice dislocation mechanisms.

The activation volumes were also estimated from the experiments using the differential stressing rate method and then calculated from:

$$V^* = \frac{RT \ln(\dot{\varepsilon}_2/\dot{\varepsilon}_1)}{\sigma_2 - \sigma_1}$$

These are also listed in Table 7. The activation volumes are all of the magnitude of 10^{-21}cc, rather large for diffusional processes.

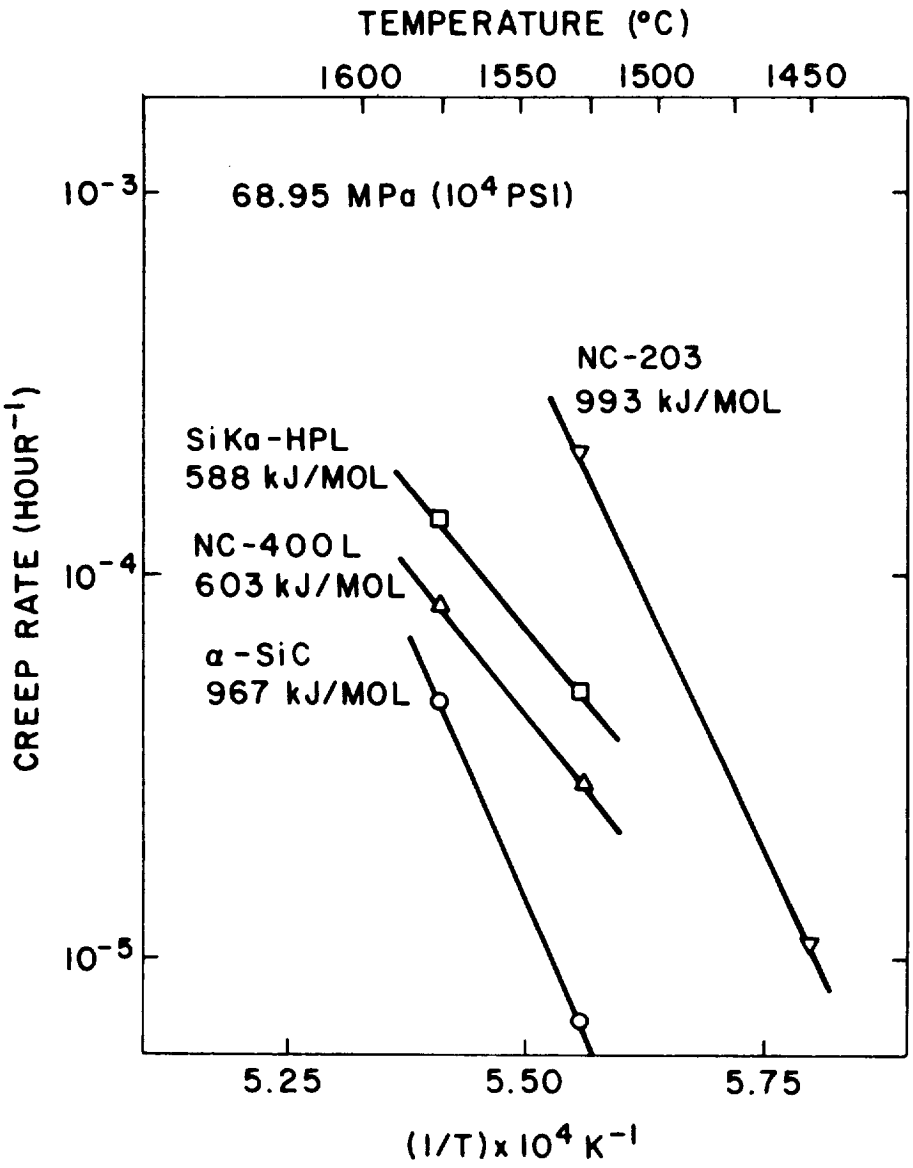

Figure 15. Creep rates and their activation energies.

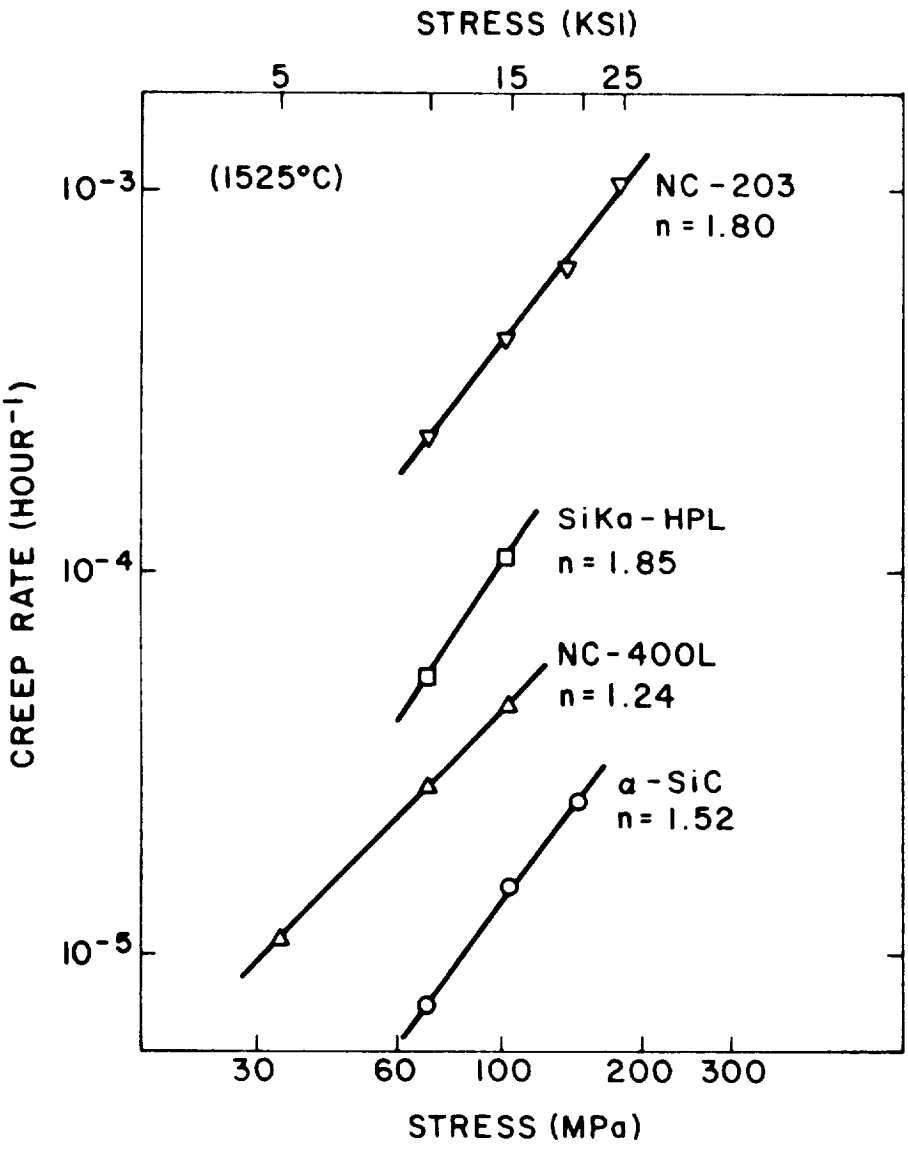

Figure 16. The creep-stress exponents of the silicon carbides.

When the creep rates, activation energies, stress exponents, and activation volumes are all considered simultaneously, it suggests that the creep process, or processes in these materials are probably related to a mechanism of flow at the grain boundaries. A natural process for this deformation is the viscous flow of the grain boundary silicates. The relatively high creep rate of the NC-203, a fine grain size hot pressed body containing substantial additives supports this interpretation.

As opposed to the other portions of this study, these creep results do not contain any commercial bodies with free Si present. This is because the free-Si containing bodies could not be justifiably measured above 1410°C, the melting point of Si. Below that temperature, the creep rates were inadequate to yield reproducible, well defined, steady state creep regions.

Table 7. Summary of Creep Results

Material	Act. Engy. (KJ/mol)	Stress Exp.	Act. Vol. (cm^3)	Remarks
Norton Hot-Pressed NC-203	993	1.80	3.0×10^{-21}	$\frac{1450 - 1525°C}{69 - 172.4\ MPa}$
Carborundum Experimental Hot-Pressed SiKa-HP-L	588	1.85	3.5×10^{-21}	$\frac{1525 - 1575°C}{69 - 137.9\ MPa}$
Norton Recrystallized Self-Bonded NC-400L	603	1.24	4.5×10^{-21}	$\frac{1525 - 1575°C}{34.5 - 103.4\ MPa}$
Carborundum Sintered Alpha - SiC	967	1.52	4.5×10^{-21}	$\frac{1525 - 1575°C}{69 - 137.9\ MPa}$

CONCLUSIONS

Although many rather specific and detailed conclusions are summarized within each of the four theses and the eight manuscripts listed as references, only the high points will be emphasized here.

1. The impact resistance, or energy obsorption during impact failure of silicon carbide is only the stored elastic strain energy in the material at fracture. There is no evidence of any plastic deformation or ductility and little additional energy dissipation during the fracture process at temperatures below 1700°C.

2. The flaw populations which determine the strength distributions of silicon carbide and nitride ceramics are transient in nature when the ceramics are exposed to oxidizing environments and subjected to applied stresses. The changes in the strength distributions appear to be the result of competing processes, some weakening and some strengthening the ceramics. Indications are that a threshold stress intensity, a K_{Ith}, may exist, below which weakening does not occur. It could be a valuable design parameter for engineering applications.

3. All silicon carbide ceramics are susceptible to subcritical, or slow crack growth. Their susceptibility increases substantially above 1000°C. It is, however, highly processing dependent, as the silicon carbide materials measured in this study exhibit distinct trends when grouped and analyzed according to processing. The most significant result is that those high strength materials with hot-pressing additives and sintering aids are also the least resistant or most susceptible to slow crack growth. It is highly probable that the same compositional additions which assist in densification are the cause for degrading resistance to the slow crack growth or fatigue processes.

4. Silicon carbide ceramics are highly creep resistant below about 1500°C, exhibiting activation parameters indicative of flow processes controlling actual creep mechanism. Analogous to the crack growth processes, it is suggested that grain boundary processes related to the densification additives are probably also responsible for the creep deformation.

REFERENCES

1. H. Abe, "Instrumented Charpy Impact Testing of Silicon Carbide", Ph.D. Thesis in Ceramic Science, The Pennsylvania State University (1976).

2. H. Abe, H.C. Chandan, and R.C. Bradt "Low Blow Charpy Impact Testing of SiC", Bull. Amer. Ceram. Soc. 57, (6), 587-591 (1978).

3. H.C. Chandan, R.C. Bradt, and G.E. Rindone "Dynamic Fatigue of Float Glass", J. Amer. Ceram. Soc. 61, (5-6), 207-210 (1978).

4. H.C. Chandan, "Elevated-Temperature Instrumented Charpy Impact Testing of Commercial and Experimental Silicon Carbide", Ph.D. Thesis in Ceramic Science, The Pennsylvania State University, (1980).

5. H.C. Chandan, L. Hermansson, H. Abe, and R.C. Bradt "Elevated Temperature Instrumented Charpy Impact of a Sintered Silicon Carbide". To be published in Ceramics International.

6. T.E. Easler, R.C. Bradt, and R.E. Tressler "Concurrent Flaw Populations in SiC" J. Amer. Ceram. Soc. 64, (3), c53-55 (1981).

7. T.E. Easler, "Environmental Effects on the Strength Distributions of Silicon Carbide and Silicon Nitride". M.S. Thesis in Ceramic Science, The Pennsylvania State University (1980).

8. T.E. Easler, R.C. Bradt, and R.E. Tressler "Strength Distributions of SiC Ceramics after Oxidation and Oxidation Under Load". J. Amer. Ceram. Soc. 64, (12), 731-734 (1981).

9. T.E. Easler, R.C. Bradt, and R.E. Tressler "Effects of Oxidation and Oxidation Under Load on Strength Distributions of Si_3N_4". J. amer. Ceram. Soc. 65, (6), 317-320 (1982).

10. M.A. Walton, "Dynamic Fatigue of SiC at Elevated Temperatures". M.S. Thesis in Ceramic Science, The Pennsylvania State University (1980).

11. M.A. Walton and R. C. Bradt "Dynamic Fatigue of Oxidized Silicon Carbides". Proc. Brit. Cer. Soc. 32, 249-260 (1982).

12. L. Hermansson and R.C. Bradt "Flexural Creep of Silicon Carbide Materials". Science of Ceramics, Vol 11, 447-452 (1981).

1. Report No.	2. Government Accession No.	3. Recipient's Catalog No.
NASA CR-165325		

4. Title and Subtitle	5. Report Date
The Impact Resistance of SiC and Other Mechanical Properties of SiC and Si_3N_4	April 1984
	6. Performing Organization Code
7. Author(s)	8. Performing Organization Report No.
Richard C. Bradt	None
	10. Work Unit No.
9. Performing Organization Name and Address	11. Contract or Grant No.
The Pennsylvania State University Dept. of Materials Science and Engineering University Park, Pennsylvania 16802	NSG-3016
	13. Type of Report and Period Covered
12. Sponsoring Agency Name and Address	Contractor Report
National Aeronautics and Space Administration Washington, D.C. 20546	14. Sponsoring Agency Code
	533-04-1C

15. Supplementary Notes

Final report. Project Manager, William A. Sanders, Materials Division, NASA Lewis Research Center, Cleveland, Ohio 44135.

16. Abstract

Studies focused on the impact and mechanical behavior of SiC and Si_3N_4 at high temperatures are summarized. Instrumented Charpy impact testing is analyzed by a compliance method and related to strength; slow crack growth is related to processing, and creep is discussed. The transient nature of flaw populations during oxidation under load is emphasized for both SiC and Si_3N_4.

17. Key Words (Suggested by Author(s))	18. Distribution Statement
Creep of SiC; Fracture statistics; Impact of ceramics; Silicon carbide; Slow crack growth of SiC; Silicon nitride; Threshold stress intensity; Impact resistance; Mechanical properties	Unclassified - unlimited STAR Category 27

19. Security Classif. (of this report)	20. Security Classif. (of this page)	21. No. of pages	22. Price*
Unclassified	Unclassified	45	A03

*For sale by the National Technical Information Service, Springfield, Virginia 22161